OpenAI Math Digest

CATALOGUE 079

Local smoothing for the Euclidean wave equation

Catalogue synthesis & 2 proof overviews

Independent reading guide · English edition

Edition: 2026-10-28
Created by: Masataka Iwai · Osaka University

> AI-generated explanations may contain errors. Check important claims and proofs against the original manuscripts. This booklet collects the website's explanations, not the original papers. Expert review and formal verification have not been performed.

Contents

The synthesis comes first, followed by all 2 overviews in official catalogue order. The contents and citations are clickable. Wide tables are arranged as entries for print; the claims and source references are retained.

00 · Catalogue synthesis 3

01 · Local smoothing for the Euclidean wave equation 9

02 · Critical local smoothing for the three-dimensional wave equation 27

Original-manuscript snapshot: `7ef5c0cc5ca4b0e072b7a050fca09ab24bc6fa3a`

Catalogue 079 · Synthesis

Read on the website ↗

CATALOGUE 079

Local smoothing for the Euclidean wave equation

Official catalogue 079 contains two manuscripts: an all-dimensional determinant-energy argument and a three-dimensional wave-packet and entropy argument. They reach a common three-dimensional local-smoothing conclusion by different methods. The first also claims a quantitative logarithmic estimate and a broad family of analytic and geometric consequences.

1. Papers in official catalogue order

These summaries give the principal scope; consult the cited original results for the complete hypotheses and statements.

Catalogue 079 · 2026-10-28 checked source snapshot

#

01

Manuscript and overview

Local smoothing for the Euclidean wave equation →

Short name: Local smoothing for the Euclidean wave equation
October 25, 2026 · 59 pages

Original paper (GitHub) ↗

Principal claim

Half-wave local smoothing in all $n \geq 2$: $[\log(2+N)]^{2/p_c}$ on a critical annulus, and order $s_+(p)+\varepsilon$ for all $2 \leq p < \infty$.

Theorems 1.1–1.2 · pp. 1, 4 ↗

Role and available overview

A conserved current, rank-one-background determinant energy and two annular comparisons. Branches to BR, restriction, Schrödinger, and Kakeya/Nikodym estimates.

Read the proof overview →

#

02

Manuscript and overview

Critical local smoothing for the three-dimensional wave equation →

Short name: Critical local smoothing for the three-dimensional wave equation
September 24, 2026 · 165 pages

Original paper (GitHub) ↗

Principal claim

Critical spacetime L^3 smoothing in three dimensions with every positive Sobolev loss; consequences for all $2 < p < \infty$, $\alpha > \max\{0, 1 - 3/p\}$.

Theorem 1.1 · p. 1; Corollary 10.6 · p. 158 ↗

Role and available overview

A route through extremal cylinder configurations and phase-record entropy, linked by thin-round transfer and regularity on the physical initial slice.

Read the proof overview →

2. Comparing the ranges and proof methods

Write $J = (1 - \Delta)^{1/2}$ and use the time interval $[1, 2]$. Complex conjugation changes the sign of the half wave, so the sign convention is not a difference in the conclusions.

Comparison

Dimensions and main range

Local smoothing for the Euclidean wave equation

All $n \geq 2$, $2 \leq p < \infty$, at Sobolev order $\max\{0, (n-1)/2 - n/p\} + \varepsilon$; no loss at $p = 2$

Critical local smoothing for the three-dimensional wave equation

$n = 3$, $p = 3$, every $\varepsilon > 0$; Corollary 10.6 gives all $2 < p < \infty$, $\alpha > \max\{0, 1 - 3/p\}$

Comparison

Critical frequency annulus

Local smoothing for the Euclidean wave equation

$[\log(2+N)]^{2/p_c}$ at $p_c = 2n/(n-1)$; the optimal logarithmic power for unrestricted data remains undetermined

Critical local smoothing for the three-dimensional wave equation

Every positive power loss; $\varepsilon = 0$ is not treated and no precise logarithmic refinement is claimed

---

Comparison

Main reduction

Local smoothing for the Euclidean wave equation

A positive current retaining interference → rank-one-background determinant problem → boundary flux → two annular comparisons

Critical local smoothing for the three-dimensional wave equation

Thin round configurations → the cylinder model; extremizers → contradiction for phase-record entropy → regularity on the physical initial slice

---

Comparison

Analytic consequences

Local smoothing for the Euclidean wave equation

All-dimensional BR and maximal BR, Stein square functions, sphere/truncated-cone/compact-paraboloid extension, Schrödinger mixed norms

Critical local smoothing for the three-dimensional wave equation

Three-dimensional maximal half waves, maximal BR and convergence, and the full strict fixed-radius BR range

Specializing the first manuscript to $n = 3$ includes the local-smoothing conclusions of Theorem 1.1 and Corollary 10.6 of the second. This is **inclusion of result ranges**. In the text and references checked, no citation or application taking the second manuscript as a proof input to the first was found. The second manuscript's quantitative inputs to its cylinder analysis are the Guth–Wang–Zhang wave-envelope theorem and the Ren–Wang planar Furstenberg theorem; these should not be mixed with the intermediate results of the determinant-energy method.

[OpenAI26EW, Theorem 1.1, p. 1] [OpenAI26EW, Theorem 1.2, p. 4] [OpenAI26CW, Theorem 1.1, p. 1] [OpenAI26CW, Corollary 10.6, p. 158]

The all-dimensional critical logarithmic estimate / The three-dimensional manuscript and its model reductions

3. What follows from local smoothing

The first manuscript uses two kinds of connections. Local spherical extension and tube maximal estimates retain the annular logarithm; the latter carry power $4/p_c$. Global restriction in the interior range, BR at strict orders, and square functions absorb a small loss. For Schrödinger evolution in d spatial dimensions, the critical $p_c = 2(d+1)/d$ estimate retains a logarithm, whereas $p > p_c$, $p \le r \le \infty$ give the exact mixed-norm order $d(1-2/p) - 2/r$.

[OpenAI26EW, Corollaries 9.1, 9.3, 12.1; Theorems 10.1, 11.1, pp. 27–29, 32, 34, 37]

The second manuscript's maximal half-wave estimate requires $3 \le p < \infty$ and $s > 1 - 2/p$: Sobolev embedding in time costs additional regularity compared with spacetime smoothing. Its maximal BR theorem has $3 \le p < \infty$ and $\delta > 1 - 3/p$. Interpolation and duality extending fixed-radius BR to all $1 \le p \le \infty$ are not applied to the maximal operator. Section 11.1 records sphere restriction and Kakeya maximal estimates through an external standard chain; the second article does not present all external inputs in that chain as checked.

[OpenAI26CW, Corollary 10.7, Theorem 11.1, Corollary 11.2, Section 11.1, pp. 160–162]

Conditions and derivations of the first manuscript's consequences / The second manuscript's maximal and BR consequences

4. Relation to catalogue 074's Kakeya manuscripts

On p. 27 the first manuscript cites, for comparison, Theorem 1.1 of The Kakeya maximal conjecture in three dimensions in catalogue 074 ($L^3(\mathbb{R}^3) \to L^3(S^2)$ with every $\delta^{-\varepsilon}$ loss), and Theorem 1.1 of Every Four-Dimensional Kakeya Set Has Full Hausdorff Dimension. At $n = 3$, its tube maximal estimate gives the fixed power $[\log(2/\delta)]^{4/3}$; at $n = 4$, it gives Hausdorff dimension four for arbitrary Kakeya sets. These compare conclusions for the same objects. The catalogue 074 results are not used as inputs to its all-dimensional wave theorem.

[OpenAI26EW, Section 9, comparison with references [62]–[63], p. 27] [OpenAI26a, Theorem 1.1, p. 2] [OpenAI26b, Theorem 1.1, p. 3]

The first manuscript passes from the tube maximal estimate to Hausdorff dimension through varying-radius covers. No reverse arrow extracts a four-dimensional Kakeya maximal estimate from the set-dimension theorem alone. No direct citation of the two catalogue 074 manuscripts was found in the second manuscript.

Elliptic capacity propagation and Fourier restriction to the sphere in catalogue 077 is a comparison on p. 29 of the first manuscript. Bochner–Riesz multipliers in three dimensions in catalogue 078 is mentioned as an alternative proof on p. 162 of the second, which explicitly says it is not an input. Both are distinct from catalogue 074.

[OpenAI26EW, Section 9.1, comparison with reference [64], p. 29]
[OpenAI26CW, Proof of Corollary 11.2, comparison with reference [20], p. 162]

5. Sources and checking scope

[OpenAI26EW] denotes the first manuscript (October 25, 2026), [OpenAI26CW] the second (September 24, 2026), [OpenAI26a] catalogue 074's three-dimensional maximal manuscript (September 23, 2026), and [OpenAI26b] its four-dimensional dimension manuscript (September 24, 2026). All are authored by OpenAI and refer to the sources at fixed commit `7ef5c0cc5ca4b0e072b7a050fca09ab24bc6fa3a`. The official subject is Real and complex analysis, on overview pp. 9–10; item 079 is on p. 9.

OpenAI Research Catalog · Catalogue 079 · p. 9

Each article records which main statements, central reductions, and bilingual conditions were compared with the sources. After the draft, an independent reviewer checked the printed statements and application hypotheses of the Gilbarg–Trudinger regularity theorems used directly in Theorem A.1 of the first manuscript, resolving the initial gap. This is not an independent reproof of the external theorems or all boundary calculations. The complete conditional-information and model-transfer lemmas in the second manuscript, and the full proofs of either manuscript, were not independently verified. Unchecked connections are distinguished both from absence of dependence and from checked comparisons of results.

079 / 01

Read on the website ↗

CATALOGUE 079 · PAPER 01 / 2 Overview

Local smoothing for the Euclidean wave equation

A determinant energy for a conserved current: from the critical logarithm to restriction and maximal estimates

The manuscript claims an annular logarithmic estimate at $p_c = 2n/(n-1)$ for the Euclidean half wave in every spatial dimension $n \geq 2$. Its central construction retains the interference in a superposition of waves, builds a positive conserved current, and uses its time component as the density of a quaternionic Hessian Dirichlet problem. This article explains the manuscript's claims and reductions; it is not an independent verification of the complete proof.

Manuscript author: OpenAI · October 25, 2026 · 59 pages, including references

Read the manuscript on GitHub ↗

1. Main results

Put $U(T) = e^{-iT|D|}$, $I = [1,2]$, $J = (1-\Delta)^{1/2}$ and $s_+(p) = \max\{0, (n-1)/2 - n/p\}$. Wave data are complex Schwartz functions, with extensions by density in the indicated spatial norms. Constants depend on the displayed dimensions, exponents, fixed cutoffs and time intervals, but not on the data or the large frequency parameter.

Theorem 1.1 — Wave local smoothing

For $n \geq 2$, $2 \leq p < \infty$ and $\varepsilon > 0$,

$$\|U(T)f\|_{L^p(\mathbb{R}^n \times I)} \leq C_{n,p,\varepsilon} \|J^{s_+(p)+\varepsilon} f\|_{L^p(\mathbb{R}^n)}.$$

At $p = 2$ one may take $\varepsilon = 0$. For $p \geq p_c$ this gains every amount strictly below $1/p$ over the fixed-time order $(n-1)(1/2 - 1/p)$; for $2 < p < p_c$ any positive regularity suffices. This theorem does not assert the lossless Sobolev endpoint for $p > 2$.

Theorem 1.1 · p. 1

Theorem 1.2 — The critical annular logarithm

For $n \geq 2$, $p = p_c$, $\varphi \in C_c^\infty(\mathbb{R}^n \setminus \{0\})$, $N \geq 2$ and $P_N = \varphi(D/N)$,

$$\|U(T)P_N f\|_{L^p(\mathbb{R}^n \times I)} \leq C_{n,\varphi}[\log(2+N)]^{2/p}\|f\|_{L^p(\mathbb{R}^n)}.$$

This is not an $L^{p_c} \to L^{p_c}_{T,X}$ bound uniform over all frequencies. The focusing example in Proposition 8.1 requires logarithmic power at least $1/p_c$, leaving a gap to the upper power $2/p_c$ for unrestricted data. Proposition 8.2 asserts that Sobolev order zero fails for $2 < p \leq p_c$ even in the weak spacetime norm.

Theorem 1.2 · p. 4 Propositions 8.1–8.2 · pp. 26–27

Corollary 9.1 — Local spherical extension and the Kakeya maximal function

Let $Eg(X) = \int_{S^{n-1}} e^{iX\cdot\omega} g(\omega)\, d\sigma(\omega)$, and let $K_\delta f(\omega)$ be the supremum of the averages of $|f|$ over all translates of a length-one, radius-δ tube in direction ω. For $n \geq 2$, $R \geq 2$, $z \in \mathbb{R}^n$ and $0 < \delta \leq 1$,

$$\|Eg\|_{L^{p_c}(B(z,R))} \leq C_n[\log(2+R)]^{2/p_c}\|g\|_{L^{p_c}(S^{n-1})},$$

$$\|K_\delta f\|_{L^n(S^{n-1})} \leq C_n[\log(2/\delta)]^{4/p_c}\|f\|_{L^n(\mathbb{R}^n)}.$$

Every subset containing a unit line segment in every direction has Hausdorff dimension n. The maximal estimate and the dimension assertion are distinct conclusions: the latter requires a covering argument with varying radii.

Corollary 9.1 · p. 27

Corollary 9.3 — Global extension for the sphere and truncated cone

Let $1 < a \leq \infty$, $b < \infty$, with a' the conjugate exponent, and assume

$$b > \frac{2n}{n-1}, \qquad b > \frac{n+1}{n-1}a'.$$

For spherical extension E and extension E_Σ from the induced surface measure on $\Sigma = \{(\rho\omega, \rho) : 1 \leq \rho \leq 2,\ \omega \in S^{n-1}\} \subset \mathbb{R}^{n+1}$,

$$\|Eg\|_{L^b(\mathbb{R}^n)} \lesssim_{n,a,b} \|g\|_{L^a(S^{n-1})}, \qquad \|E_\Sigma G\|_{L^b(\mathbb{R}^{n+1})} \lesssim_{n,a,b} \|G\|_{L^a(\Sigma)}.$$

These are strong estimates, including $a = \infty$. For $b = \infty$, both hold for every $1 \leq a \leq \infty$. The boundaries of the two strict inequalities for finite b are excluded.

Corollary 9.3 · pp. 28–29

Theorem 10.1 — Bochner–Riesz means, the maximal function and convergence

Put $B_r^\alpha = (1-|D|^2/r^2)_+^\alpha$, $B_*^\alpha f = \sup_{r>0}|B_r^\alpha f|$ and $\delta(p) = \max\{0, n|1/p-1/2|-1/2\}$. If $n \geq 2$, $1 \leq p \leq \infty$ and $\alpha > \delta(p)$, then

$$\sup_{r>0} \|B_r^\alpha f\|_p \leq C_{n,p,\alpha}\|f\|_p.$$

For $p < \infty$, $B_r^\alpha f \to f$ in L^p as $r \to \infty$. Moreover, for $2 \leq p < \infty$ and $\alpha > s_+(p)$,

$$\|B_*^\alpha f\|_p \leq C_{n,p,\alpha}\|f\|_p,$$

and $B_r^\alpha f \to f$ almost everywhere. The fixed-radius range $1 \leq p < 2$ is not asserted for the maximal operator.

Theorem 10.1 · p. 32

Theorem 11.1 — Stein's square function

$$G^\alpha f(x) = \left(\int_0^\infty |r\partial_r B_r^\alpha f(x)|^2 \frac{dr}{r}\right)^{1/2}.$$

For $n \geq 2$, $2 \leq p < \infty$ and $\alpha > \max\{1/2, n(1/2-1/p)\} = 1/2 + s_+(p)$, one has $\|G^\alpha f\|_p \leq C_{n,p,\alpha}\|f\|_p$. The assertion includes extension from Schwartz data to L^p.

Theorem 11.1 · p. 34

Corollary 12.1 — The compact paraboloid and Schrödinger local smoothing

In this result write $d \geq 1$ for spatial dimension, $p_c = 2(d+1)/d$, B^d for the unit ball, and $\mathcal{E}g(x,t) = \int_{B^d} e^{i(x\cdot v + t|v|^2)} g(v)\,dv$.

If $1 < a \leq \infty$, $p_c < b < \infty$ and $b > (d+2)a'/d$, then

$$\|\mathcal{E}g\|_{L^b(\mathbb{R}^{d+1})} \lesssim_{d,a,b} \|g\|_{L^a(B^d)}.$$

For a compact time interval $I \subset \mathbb{R}$, $N \geq 2$ and Schwartz f with $\operatorname{supp}\widehat{f} \subset B(0,N)$,

$$\|e^{it\Delta}f\|_{L^{p_c}(\mathbb{R}^d \times I)} \lesssim_{d,I} [\log(2+N)]^{2/p_c}\|f\|_{p_c}.$$

For $p_c < p < \infty$, $p \leq r \leq \infty$ and arbitrary Schwartz data, setting $s = d(1-2/p) - 2/r$ gives

$$\|e^{it\Delta}f\|_{L^p(\mathbb{R}^d;L^r(I))} \lesssim_{d,p,r,I} \|f\|_{B^s_{p,p}(\mathbb{R}^d)} \lesssim_{d,p,s} \|(1-\Delta)^{s/2}f\|_p.$$

Thus $r=p$ gives the exact spacetime Sobolev order $d-2(d+1)/p$, and $r=\infty$ gives the maximal estimate on the same finite time interval. This does not include a logarithm-free estimate at $p=p_c$.

Corollary 12.1 · p. 37

References on the arrows

Unprefixed theorem, lemma, section and equation numbers refer to Local smoothing for the Euclidean wave equation. External inputs use the following keys.

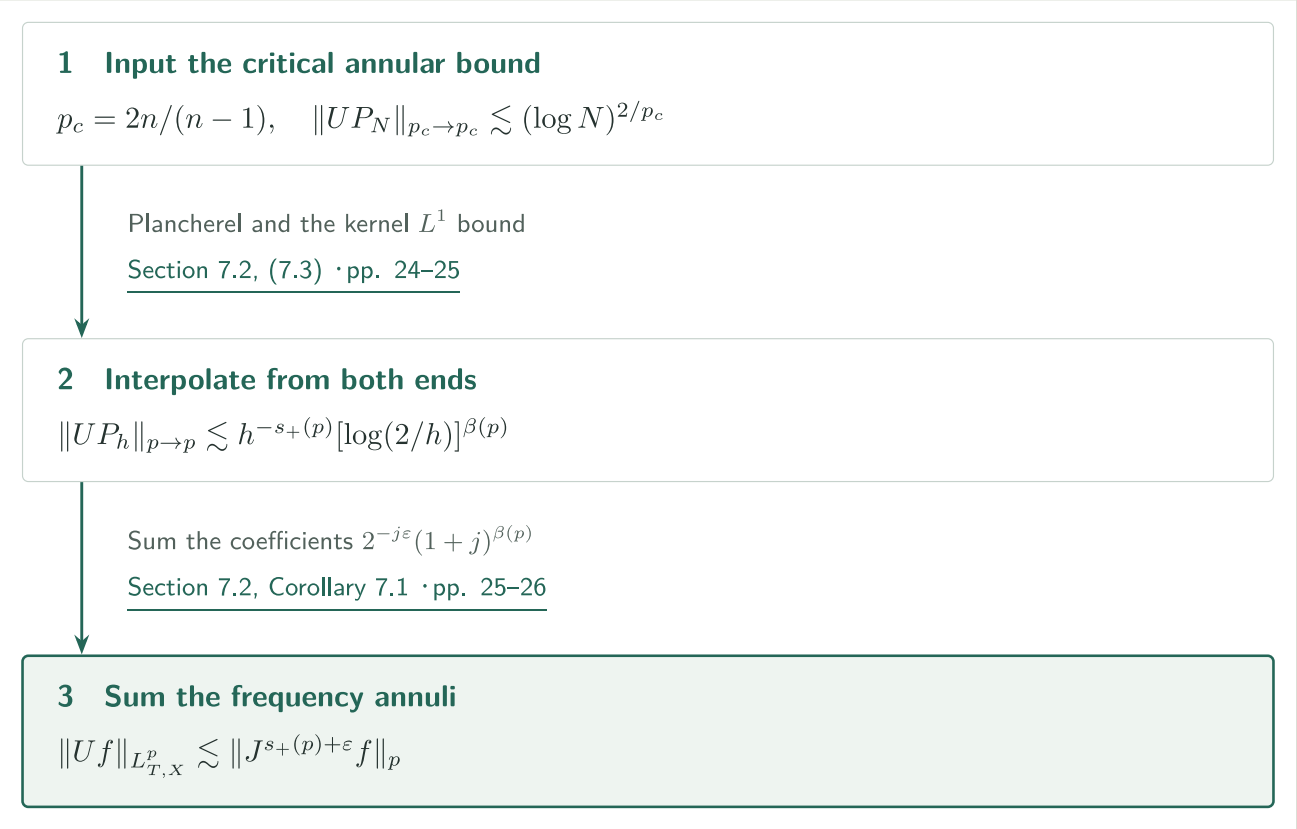
- Tao99 Terence Tao — The Bochner-Riesz conjecture implies the restriction conjecture: Epsilon removal from local spherical restriction to global estimates. Author-hosted undated preprint; accessed October 28, 2026 (DVI converted to PDF).
- Kim17 Jongchon Kim — Some remarks on Fourier restriction estimates: Epsilon removal on compact hypersurfaces with Fourier decay. arXiv:1702.01231v2, February 9, 2017.
- LRS13 Sanghyuk Lee, Keith M. Rogers, Andreas Seeger — On space-time estimates for the Schrödinger operator: Diagonal extension implies mixed-norm bounds at the exact Besov order. arXiv:1108.1518v2, March 19, 2012; published 2013.
- GT01 David Gilbarg, Neil S. Trudinger — Elliptic Partial Differential Equations of Second Order: Direct input for periodic-fiber Dirichlet invertibility and boundary/interior regularity. Theorems 6.14 (printed p. 107), 6.19 (p. 111), 17.14 (p. 461), 17.26′ (p. 481), and structural conditions (p. 456) were independently checked after the draft; the external proofs were not verified. Classics in Mathematics, Springer, 2001; reprint of the 1998 edition (bibliography [31] of the manuscript).

Each citation gives the result and pages. When printed pagination differs from the PDF position, both are shown. GitHub previews do not automatically jump to the cited page.

2. Theorem 1.1 — From the critical annulus to all exponents

Proof target : Theorem 1.1 · p. 1

Proof route. First obtain Theorem 1.2, interpolate on either side with L^2 conservation and the fixed-time L^∞ kernel estimate, and spend ε on the frequency sum. The next section explains the critical estimate itself.



Interpolation and Sobolev summation

Open figure ↗ TeX source ↓

1. Interpolation at the two ends

With $h = N^{-1}$, Plancherel gives a uniform $L^2_X \to L^2_{T,X}$ bound, while $L^\infty_X \to L^\infty_{T,X}$ costs $O(h^{-(n-1)/2})$. For the latter, split into caps of width $h^{1/2}$ and remove the linear phase; each remaining kernel has uniformly bounded L^1 norm. Riesz–Thorin yields

$$\|UP_h f\|_{L^p_{T,X}} \lesssim h^{-s_+(p)}[\log(2/h)]^{\beta(p)}\|f\|_p, \quad \beta(p) = \min\{(n-1)(1-2/p), 2/p\}.$$

Section 7.2, (7.3) · pp. 24–25

2. Spending the positive loss on summation

For $g = J^{s_+(p)+\varepsilon} f$, the coefficient on the jth annulus is $2^{-j\varepsilon}(1+j)^{\beta(p)}$, an absolutely summable sequence. Mihlin handles low frequencies; Plancherel directly gives the lossless $p = 2$ case. Corollary 7.1 refines this sum to logarithmic Sobolev bounds with $B > \beta(p) + 1/2 - 1/p$ (or equality with an additional iterated-logarithm condition), but does not generally give $B = C = 0$.

Section 7.2, Corollary 7.1 · pp. 25–26

3. Theorem 1.2 — The conserved current and two annular comparisons

Proof target : Theorem 1.2 · p. 4

Proof route. Lift a cap-localized wave on a fixed torus to a conserved current. A determinant equation on spatial fibers produces an energy detecting the p_cth power. Gaussian decay at the wall yields a nonnegative scalar supersolution; two annular comparisons then give the logarithm, after which the spatial period is removed.



The conserved current and the critical logarithm

Open figure ↗ TeX source ↓

1. Preserving interference and producing the critical power

Two auxiliary flows of a symmetric first-order system produce $A_0 = \chi\chi^*$. The vector χ is formed by **summing** the Gaussian-weighted waves before taking the square. Every real column is divergence free, and $(\partial\Phi)A_0 = 0$. For frequency $N = h^{-1}$ in a fixed small cap, the time component recovers the wave when the auxiliary radius is comparable to h.

The fiber defining function satisfies $H_{\mathrm{fib}}(r) > 0$. The null line of the full $H(r)$ is orthogonal both to the boundary normal and to the image of $H(|\Phi|^2)$. Smooth and cut off the current, then add a small cofactor current to obtain $\mu = A_{TT} > 0$. For $B_0 = \lambda|\Phi|^2$, $\lambda = h^{-30n}$, solve

$$\det H_{\mathrm{fib}}(B_0 + u) = \lambda\mu, \qquad u|_{\partial\Omega_z} = 0, \qquad H_{\mathrm{fib}}(B_0 + u) > 0.$$

The positive defining Hessian and density gap satisfy Theorem A.1. The spatial background has rank one, so $\det(B_{\mathrm{fib}} + \alpha I) = (\beta + \alpha)\alpha^{n-1}$ with $\beta \asymp \lambda$. A density lower bound m on a small ball forces $-u \gtrsim h^2 m^{1/(n-1)}$; consequently $(-u)\mu$ detects $m^{n/(n-1)}$, hence the wave's $2n/(n-1)$ power.

Proposition 2.2, (2.15), Lemma 4.1 · pp. 9–10, 14 Section 4.2, Theorem A.1 · pp. 15, 38–41

2. Cancelling the indefinite determinant, retaining only boundary flux

The Laplacian of $X_0 = \int_{\Omega_z}(-u)\mu$ contains a full determinant of uncontrolled sign. Correct it by

$$F = X_0 + \lambda^{-1}\int_{\Omega_z} u \int_0^1 \det H_{\mathrm{fib}}(B_0 + \theta u)\, d\theta.$$

Integration by parts with the two conservation laws, for the current and the Hessian cofactor, cancels that determinant. The null line makes the cofactor's normal–normal coefficient vanish, including on the moving boundary. Proposition 4.2 identifies $\Delta F + \int A : \Sigma$ with the wave's boundary flux, with $A, \Sigma \geq 0$. Lemma 4.3 gives

$$\frac{n-1}{n+1} X_0 \leq F \leq \frac{n}{n+1} X_0,$$

so the correction retains the required quantity.

Proposition 4.2, Lemma 4.3 · pp. 16–18

3. Comparing decay at the wall with recovery in the interior

Write $z = (T, \tau) \in \mathbb{R} \times \mathbb{R}^2$ and $a = Kh$. The flux-carrying wall stays a fixed angular distance from the cap, giving Gaussian decay $e^{-c_0|\tau|/h}$. Inverting the interior multiplier costs $e^{C\gamma^2|\tau|/h}$. Choose the aperture γ small first, then the fixed K large, so the wall decay dominates. The comparison function and small-ball determinant comparison yield Proposition 5.1:

$$F(0,\tau) \lesssim a^2 \|f\|_{p_c}^{p_c} \ (|\tau| = 4a), \qquad F(T,\tau) \gtrsim a^2 \|U(T)f\|_{p_c}^{p_c} \ (|\tau| = 2a),$$

$$\Delta_{T,\tau} F \le V(|\tau|) F, \qquad V(s) = C s^{-2} e^{-cs/h}.$$

The comparison uses a density lower bound throughout the small ball and the ceiling $\mu^{1/(n-1)} \le \lambda$.

Proposition 5.1, (5.11)–(5.12) · pp. 18–21

4. Accounting for both logarithms and removing the period

Let $H(T, s)$ be the circular mean of F at $|\tau| = s$. Lemma 6.1 with $b = 2a$, $r = 2b$ gives

$$H(0, 2b) \gtrsim [\log(3/b)]^{-2} \int_1^2 H(T, b)\, dT.$$

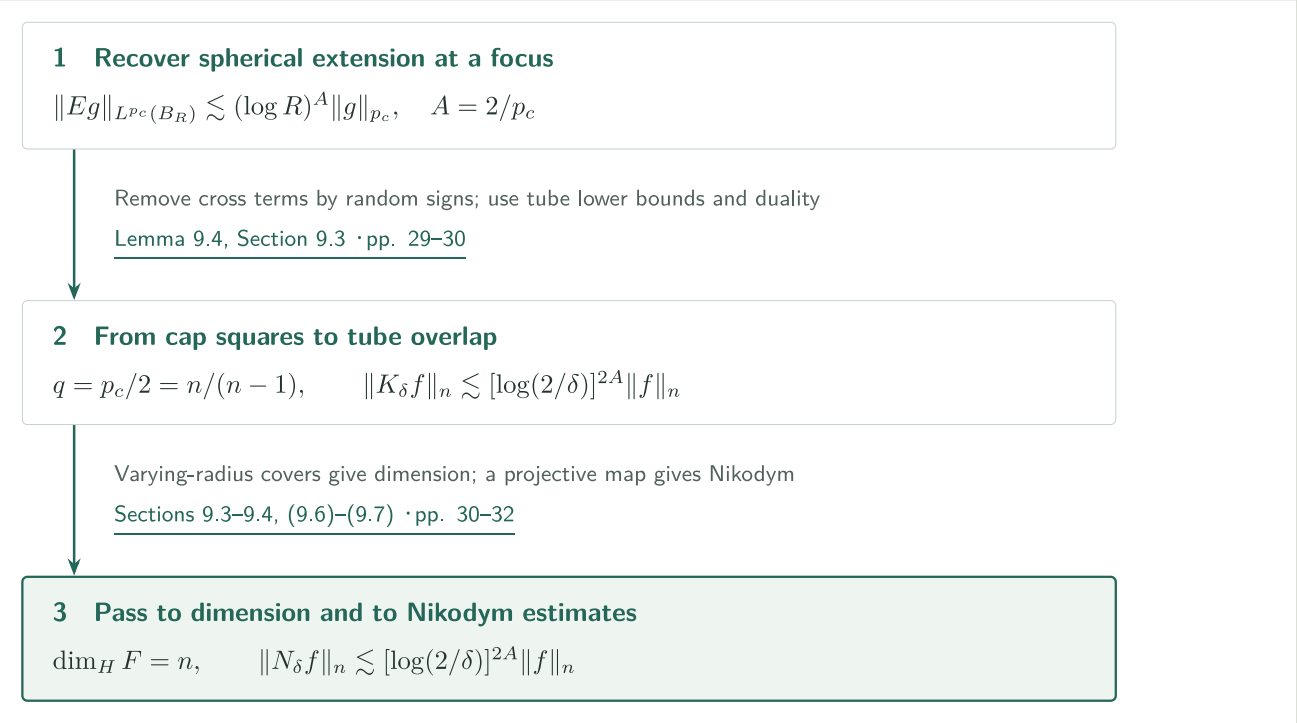
The steps are an outward annular comparison, a mean inequality at fixed radius, and an inward comparison. A radial planar harmonic function is affine in $\log s$, so each passage costs one inverse logarithm. Exponential decay uniformly bounds the weighted integral of the positive potential. Cancel the factors a^2 and take p_cth roots to obtain Proposition 6.3. Sum a fixed finite family of caps. Outside $|X| \ge 3$, nonstationary phase bounds the wave kernel by $O(h^M (1 + |X|)^{-M})$. Local periodization on unit cubes and bounded overlap then transfer the estimate to $\mathbb{R}^n$.

Lemma 6.1, Proposition 6.3 · pp. 21–23 Section 7.1 · p. 24

4. Corollary 9.1 — From focusing to tubes and Hausdorff dimension

Proof target : Corollary 9.1 · p. 27

Proof route. Keep the wave logarithmic power as A. Local spherical extension retains A, whereas tube overlap and the Kakeya maximal operator carry $2A$. Here $A = 2/p_c$.



Spherical extension, tube maximal estimates and dimension

Open figure ↗ TeX source ↓

1. Recovering local extension near a focus

The time average $M_N f = \int \psi(T) e^{iNT} U(T) \chi(|D|/N) f \, dT$ selects a frequency shell of width one. Its leading kernel is $cN^{(n-1)/2} |Z|^{-(n-1)/2} e^{iN|Z|} \psi(|Z|)$. Insert $f_N(r\omega) = e^{-iNr} \psi(r) g(\omega)$ and linearize the distance phase at X/N near the focus. Taking N to be a sufficiently large fixed power of R bounds the error, while $n/p_c = (n-1)/2$ cancels the scaling factor. Only $\log N \asymp \log R$ remains.

Lemma 9.2 · p. 28

2. Randomizing caps and dualizing the maximal function

Modulated disjoint δ-caps have extension bounded below on tubes of length δ^{-2} and width δ^{-1}. Independent signs turn the expected square into the sum of the squared cap extensions, which bounds a weighted sum of tube indicators from below. Combining this with local extension gives Lemma 9.4's overlap estimate at $q = p_c/2 = n/(n-1)$. Grouping tube centers into cubes keeps the constant uniform for arbitrary locations. A δ-net of directions, L^n–L^q duality and the supremum over centers give the Kakeya maximal estimate.

Lemma 9.4, Section 9.3 · pp. 29–30

3. Varying-radius covers and the projective Nikodym argument

A single scale only gives $|F_\delta| \gtrsim [\log(1/\delta)]^{-2(n-1)}$. Hausdorff dimension requires grouping a cover by balls of different radii. Section 9.3 obtains infinite Hausdorff measure for the gauge $r^n[\log(1/r)]^{2(n-1)}[\log\log(1/r)]^\gamma$, $\gamma > n-1$, hence full dimension.

In Section 9.4, $N_\delta f(x)$ is the supremum of tube averages over unit segments through x, and

$$\|N_\delta f\|_{L^n(\mathbb{R}^n)} \lesssim_n [\log(2/\delta)]^{4/p_c}\|f\|_{L^n(\mathbb{R}^n)}.$$

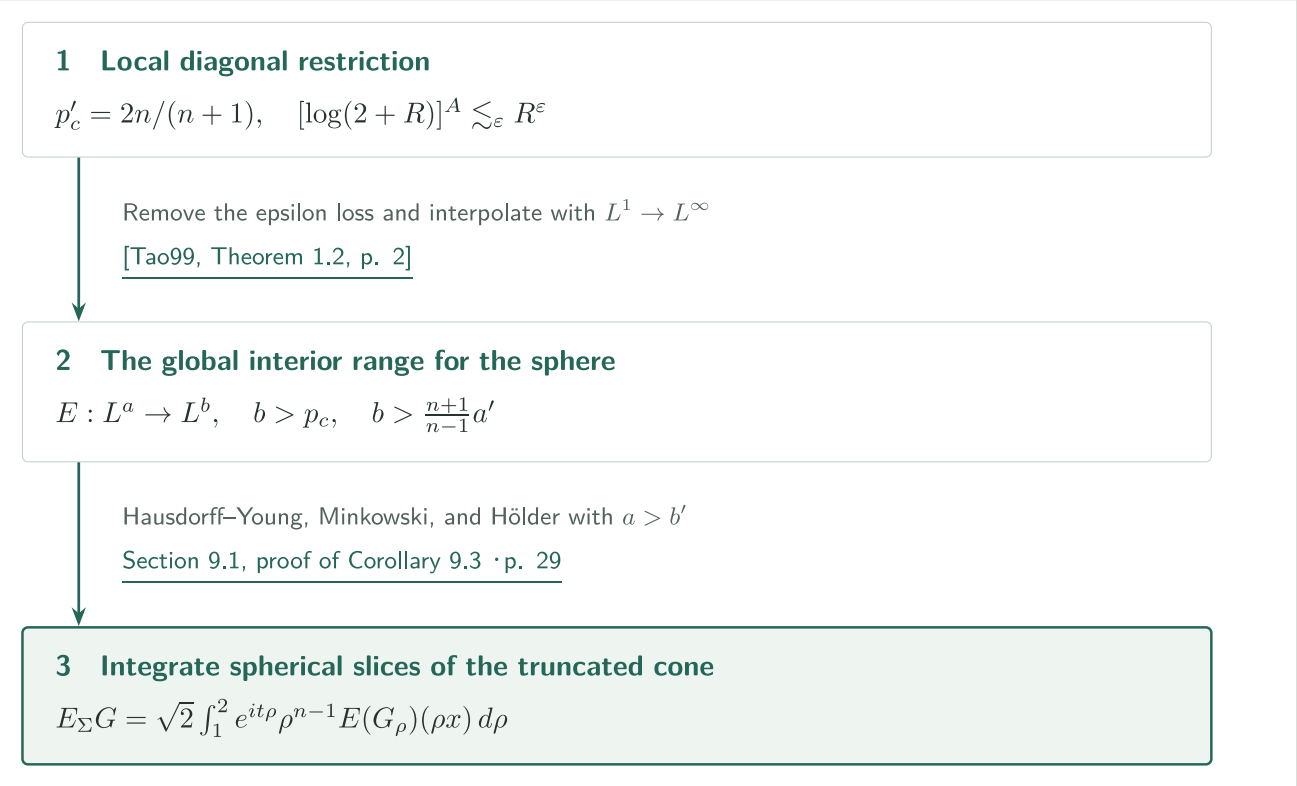
A projective map sends portions a fixed distance from the base point into tubes whose direction records that base point; its Jacobian is locally bounded above and below. Pieces near the base point are summed by dyadic distance s with weight $O(s)$. The same covering argument gives dimension n for a Borel set meeting a suitable unit segment through every point of a positive-measure set in uniformly positive length. No converse implication from dimension alone to a maximal estimate is asserted.

Sections 9.3–9.4, (9.6)–(9.7) · pp. 30–32

5. Corollary 9.3 — Epsilon removal and cone slices

Proof target : Corollary 9.3 · pp. 28–29

Proof route. Turn the local diagonal spherical bound into a global estimate at strictly larger output exponents, interpolate to the interior range, then integrate spherical slices of the cone.



Epsilon removal for the sphere and slicing the cone

Open figure ↗ TeX source ↓

1. Removing the loss and interpolating exponents

The inequality $[\log(2+R)]^A \lesssim_\varepsilon R^\varepsilon$ and duality give local $L^{p_c'} \to L^{p_c'}$ restriction. Since $1 < p_c' < 2$, [Tao99] applies. Duality gives $E : L^s \to L^s$ for every $s > p_c$. When $a \geq b$, use the finite measure of the sphere. When $a < b$, set $s = 1 + b/a'$ and interpolate with $L^1 \to L^\infty$; the hypothesis $b > (n+1)a'/(n-1)$ guarantees $s > p_c$.

Section 9.1, proof of Corollary 9.3 · p. 29 [Tao99, Theorem 1.2, p. 2]

2. Integrating the cone slices

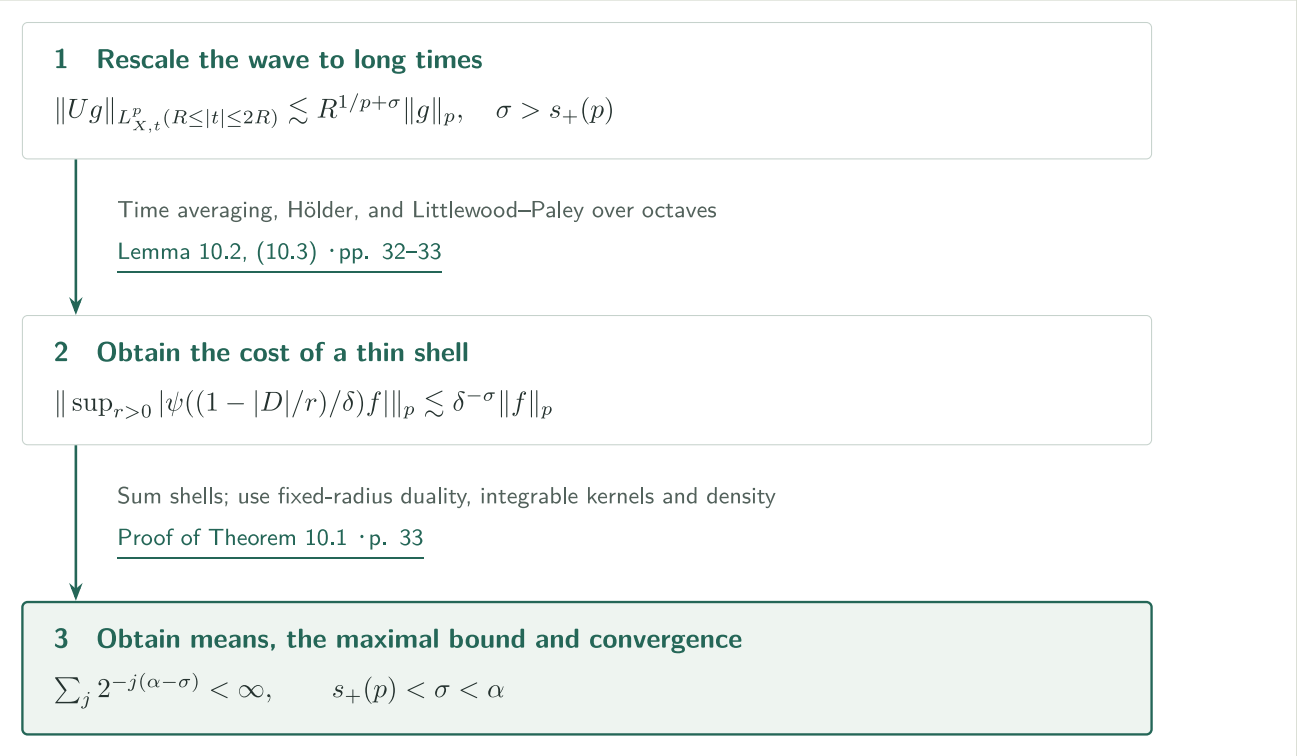
For $G_\rho(\omega) = G(\rho\omega, \rho)$, $E_\Sigma G = \sqrt{2}\int_1^2 e^{it\rho}\rho^{n-1}E(G_\rho)(\rho x)\,d\rho$. Apply Hausdorff–Young in time, Minkowski using $b \geq b'$, and spatial dilation. The final $L^{b'}_\rho$ norm is controlled by L^a_ρ because $a > b'$, which follows from the stated hypotheses. For $b = \infty$, Hölder directly bounds the defining integrals on both compact surfaces.

Section 9.1, proof of Corollary 9.3 · p. 29

6. Theorem 10.1 — Summing thin-shell maximal estimates

Proof target : Theorem 10.1 · p. 32

Proof route. Rescale to unit frequency and long wave times, express a shell as a time average, and sum shell thicknesses. Duality and density then supply the remaining conclusions.



Thin shells, Bochner–Riesz estimates and convergence

Open figure ↗ TeX source ↓

1. The time average costs an inverse power of shell thickness

For $\sigma > s_+(p)$, $2 \le p < \infty$ and g in a fixed frequency annulus, $\|U(t)g\|_{L^p(\mathbb{R}^n\times\{R\le|t|\le 2R\})} \lesssim R^{1/p+\sigma}\|g\|_p$. Fourier inversion writes $A_{\delta,r} = \psi((1-|D|/r)/\delta)$ as $\delta r \int e^{itr}\widehat{\psi}(\delta r t)U(t)g\,dt/(2\pi)$. Time Hölder and the long-time estimate bound the supremum on $r \in [1,2]$ by $O(\delta^{-\sigma})$. Dyadic radius octaves and Littlewood–Paley for $p \ge 2$ give the supremum over all radii.

Lemma 10.2, (10.3) · pp. 32–33

2. Strict order and three extensions

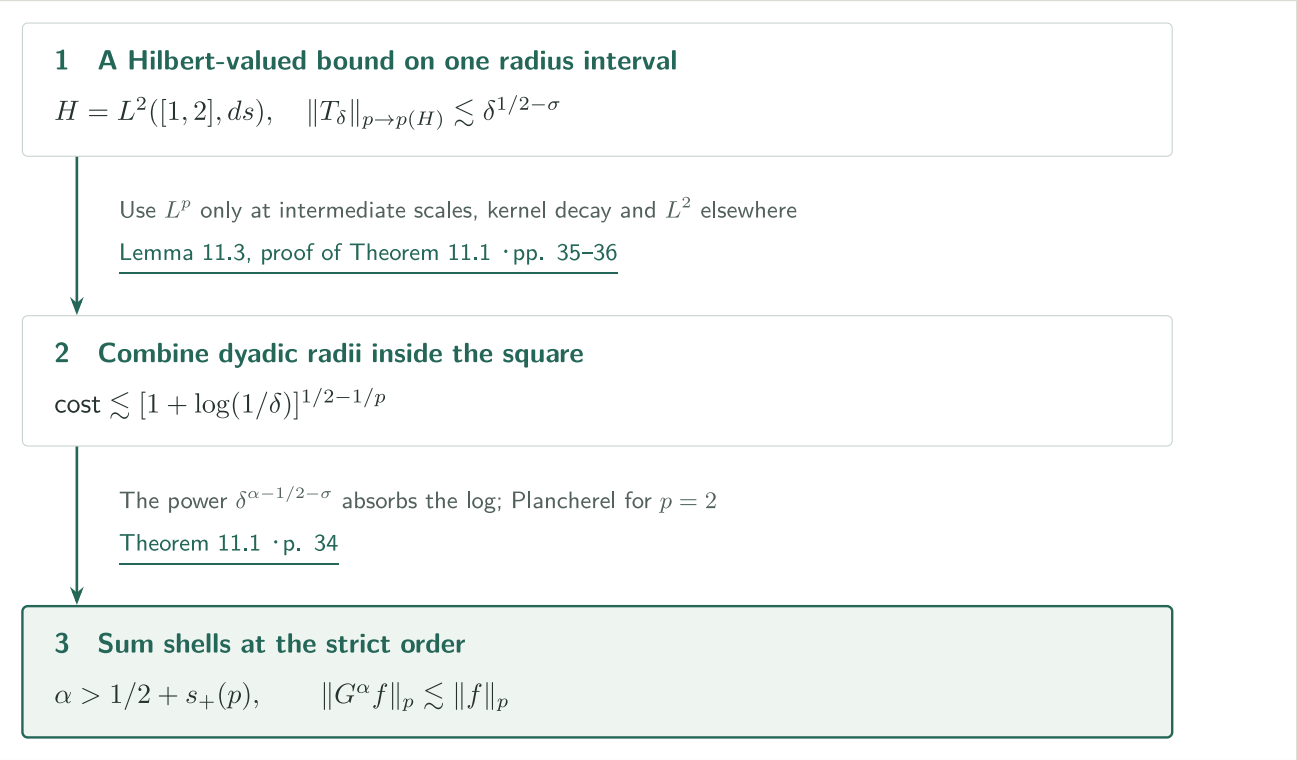
Choose $s_+(p) < \sigma < \alpha$. Splitting the multiplier near its boundary into shells of thickness $\delta = 2^{-j}$ costs $\sum_j \delta^{\alpha-\sigma}$; the smooth remainder is controlled by the Hardy–Littlewood maximal function. This proves the maximal bound and the fixed-radius bound for $p \ge 2$. Self-adjointness gives the latter for $1 < p < 2$; the integrable Bessel kernel gives $p = 1, \infty$. Convergence for Schwartz functions with compact Fourier support and density give L^p convergence. In the maximal range $2 \le p < \infty$, almost-everywhere approximation uniform in r gives pointwise convergence.

Proof of Theorem 10.1 · p. 33

7. Theorem 11.1 — Combining radii inside the square norm

Proof target : Theorem 11.1 · p. 34

Proof route. Recover $\delta^{1/2}$ on one radius interval, then use a Hilbert-valued estimate to combine all dyadic intervals inside the square norm.



Shell square estimates and Stein's square function

Open figure ↗ TeX source ↓

1. Three powers: differentiation, the square norm and smoothing

On a shell of thickness δ, radial differentiation costs $\delta^{\alpha-1}$, the square integral restores $\delta^{1/2}$, and the wave costs $\delta^{-\sigma}$. Lemma 11.2 combines Plancherel in the radius variable with the long-time wave estimate. For $H = L^2([1,2], ds)$, the shell operator has $L^p \to L^p(H)$ norm $O(\delta^{1/2-\sigma})$ and $L^2 \to L^2(H)$ norm $O(\delta^{1/2})$.

Lemma 11.2 · p. 34

2. Combining different scales inside the square

Lemma 11.3 combines dilates under decay bounds for a Hilbert-valued kernel and its first derivative. On a test cube, only $O(1+\log(1/\delta))$ intermediate scales use the L^p bound; Hölder costs $[1+\log(1/\delta)]^{1/2-1/p}$. Distant scales use a kernel derivative or L^2. Choosing $\sigma < \alpha - 1/2$

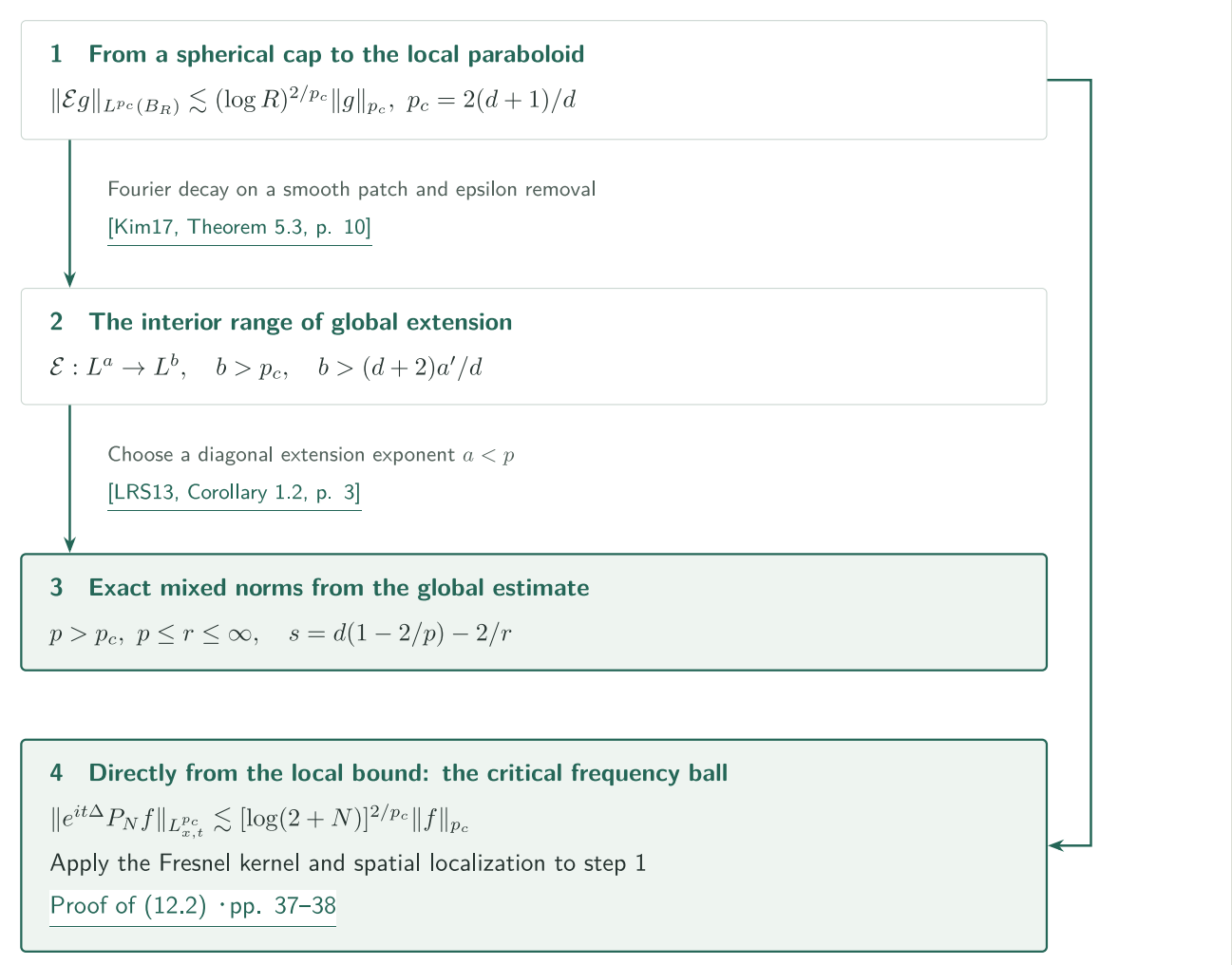
leaves $\delta^{\alpha-1/2-\sigma}$, absorbing this logarithm. The multiplier away from the boundary vanishes quadratically at zero, giving another summable series. For $p=2$, directly $\|G^\alpha f\|_2^2 = \alpha(2\alpha-1)^{-1}\|f\|_2^2$. Fatou and monotone convergence pass from finite sums to the full operator, and density extends the linear map into $L_x^p(L^2(dr/r))$.

Lemma 11.3, proof of Theorem 11.1 · pp. 35–36

8. Corollary 12.1 — The paraboloid limit and the Fresnel transform

Proof target : Corollary 12.1 · p. 37

Proof route. Rescale a spherical cap in dimension $n=d+1$ to the paraboloid while retaining the critical local logarithm. Distinguish three exits: epsilon removal, the Fresnel kernel, and an external mixed-norm theorem.



Three consequences of the local paraboloid estimate

Open figure ↗ TeX source ↓

1. The interior range of paraboloid extension

Parametrize the cap by $(\delta v, \sqrt{1-\delta^2|v|^2})$ and rescale physical variables to $(x/\delta, -2t/\delta^2)$. The new phase is $q_\delta(v) = 2(1-\sqrt{1-\delta^2|v|^2})/\delta^2 = |v|^2 + O(\delta^2)$. At $p_c = 2(d+1)/d$, the Jacobian and input powers cancel. Taking δ to be a fixed negative power of R preserves $[\log(2+R)]^{2/p_c}$ in the local estimate (12.4). For [Kim17]'s compact-surface epsilon removal, stationary phase gives Fourier decay of a smooth density on a slightly larger patch. Duality and interpolation then give the interior range in (12.1).

Proof of Corollary 12.1, (12.4) · pp. 36–37 [Kim17, Theorem 5.3, p. 10]

2. The critical Schrödinger estimate retains a logarithm on a frequency ball

Localize frequency-ball data to spatial cubes of side N. Treat distant input by nonstationary phase for $S(t)P_N$. For the nearby input $h = f1_{30Q}$, the Fresnel kernel expresses the wave through $\mathcal{E}[g](-\lambda x/(2t), \lambda^2/(4t))$, where $g(v) = h(\lambda v)$ and $\lambda \asymp N$. Keep the multiplier outside, as $P_N S(t)h$, because the spatial truncation creates high frequencies. On $t \in [1/2, 1]$, the Jacobian and input norm leave $\lambda^{d-(2d+2)/p_c} = 1$, so only the logarithm in (12.4) remains. Bounded overlap of cubes, dyadic time intervals and conjugation give any compact I.

Proof of (12.2) · pp. 37–38

3. Exact mixed-norm order strictly above the critical exponent

Choose $p_c < a < p$. Equation (12.1) gives $\mathcal{E} : L^a \to L^a$. Apply [LRS13, Corollary 1.2] with $p_0 = q_0 = a$ and both spatial exponents equal to p. This gives $B^s_{p,p} \to L^p_x L^r_t$ at exactly $s = d(1-2/p) - 2/r$ for $p \le r \le \infty$. Littlewood–Paley and $\ell^p \le \ell^2$ for $p > 2$ give the Sobolev input bound. The room to choose $a < p$ distinguishes this conclusion from the critical logarithmic estimate.

Proof of (12.3) · p. 38 [LRS13, Corollary 1.2, p. 3]

9. Which papers supply which steps

Source and result

Tao's epsilon-removal theorem

Used at

Corollary 9.3, p. 29

Role and required hypotheses

Local spherical restriction at $1 < p_c' < 2$ gives global restriction at smaller input exponents

Checking scope

Theorem 1.2, p. 2 of the author's DVI and its application checked; the full external proof not verified

---

Source and result

Kim's compact-surface form

Used at

Corollary 12.1, p. 37

Role and required hypotheses

A smooth compact patch with Fourier decay, $1 \le p \le q \le 2$, and arbitrarily small local losses

Checking scope

arXiv v2 Theorem 5.3, p. 10 and the application checked

Source and result

Lee–Rogers–Seeger's mixed-norm consequence

Used at

(12.3), p. 38

Role and required hypotheses

Diagonal extension at $a < p$, $p \le r \le \infty$, exact Besov order

Checking scope

arXiv v2 Corollary 1.2, p. 3 and the exponent substitution checked

Source and result

Gilbarg–Trudinger [GT01], elliptic regularity

Used at

Theorem A.1, pp. 39–41

Role and required hypotheses

Theorems 6.14 (printed p. 107)/6.19 (p. 111) give linear Dirichlet invertibility and higher regularity. Theorems 17.14 (p. 461)/17.26′ (p. 481) give interior/boundary $C^{2,\alpha}$ bounds from uniform ellipticity and concavity on the solution Hessian range (p. 456)

Checking scope

An independent reviewer checked the printed statements, application hypotheses, and finite-chart reduction on periodic fibers after the draft. This is not a reproof of GT or all boundary calculations

[Tao99, Theorem 1.2, p. 2] [Kim17, Theorem 5.3, p. 10] [LRS13, Corollary 1.2, p. 3]

The main proof does not take the estimate in the second paper, Critical local smoothing for the three-dimensional wave equation, as an input. The three-dimensional Kakeya maximal manuscript and four-dimensional Hausdorff-dimension manuscript in catalogue 074 are cited for comparison on p. 27. The spherical restriction manuscript in catalogue 077 is likewise a comparison on p. 29, not an input to the all-dimensional main theorem. Shell lemmas for Bochner–Riesz and square functions, cone slicing, and randomized caps are proved within this manuscript; historical citations are not automatically counted as separate proof inputs.

Sections 9–9.1 · pp. 27–29

10. Return to the sources

- Theorem 1.2 · p. 4 — The quantitative core and its logarithmic loss
- Proposition 4.2, Lemma 4.3 · pp. 16–18 — Cancellation of the indefinite full determinant and boundary flux
- Proposition 5.1, (5.11)–(5.12) · pp. 18–21 — Gaussian decay at the wall versus interior wave recovery
- Lemma 6.1, Proposition 6.3 · pp. 21–23 — The two logarithms from two annular passages
- Sections 9.3–9.4, (9.6)–(9.7) · pp. 30–32 — Separate the maximal estimates from the Hausdorff-dimension argument

- Theorem 10.1 · p. 32 — The distinct ranges for fixed radii, the maximal function and convergence
- Lemma 11.3, proof of Theorem 11.1 · pp. 35–36 — Combining radius intervals inside the square norm
- Corollary 12.1 · p. 37 — Paraboloid extension, the critical logarithm and exact mixed norms
- Section 4.2, Theorem A.1 · pp. 15, 38–41 — The periodic-fiber Dirichlet problem and external regularity whose input hypotheses were checked after the draft

The statements of Theorems 1.1/1.2, Corollaries 9.1/9.3/12.1 and Theorems 10.1/11.1, the reductions described above in Sections 2–7 and 9–12, and Appendix A's Dirichlet construction were read. After the draft, an independent reviewer compared the statements and application hypotheses of the GT regularity theorems used directly in Appendix A with the printed source, resolving the initial reservation. The full current-coordinate calculations, all cofactor components, the proofs of the GT theorems themselves, all boundary calculations in Theorem A.1, and the complete proofs in Appendices B–E were not independently verified. Propositions 8.1–8.2 were checked as statements to distinguish lossless endpoints; the focusing calculation in the former was read. Appendix B's angular regularity, the planar linear Dirichlet method, general symmetric systems, and derived statements for curve families are outside this article's detailed coverage.

079 / 02

Read on the website ↗

CATALOGUE 079 · PAPER 02 / 2 Overview

Critical local smoothing for the three-dimensional wave equation

From entropy contradictions in cylinder models to regularity on the physical initial slice and critical L^3 smoothing

The manuscript derives the critical estimate for the three-dimensional Euclidean half-wave from packet masses and multiscale phase information. It incorporates planar incidence bounds and a lower-dimensional wave-envelope estimate into cylinder models, transfers thin round configurations to those models, and connects initial regularity and terminal packet masses to the physical L^3 norm.

Manuscript author: OpenAI · September 24, 2026 · 165 pages, including references

Read the manuscript on GitHub ↗

1. Main results

Write $Uf(x,t) = e^{it|D|}f(x)$ and $J^s = (1-\Delta)^{s/2}$. Constants below may depend on the stated exponents, but not on the input function.

Theorem 1.1 — Critical local smoothing in three dimensions

For every $\varepsilon > 0$ there is a finite C_ε such that every $f \in \mathcal{S}(\mathbb{R}^3)$ satisfies

$$\|Uf\|_{L^3(\mathbb{R}^3\times[1,2])} \le C_\varepsilon \|J^\varepsilon f\|_{L^3(\mathbb{R}^3)}.$$

The lossless assertion $\varepsilon = 0$ is not included.

Theorem 1.1 · p. 1

Corollary 10.6 — The full strict positive-regularity range

For $2 < p < \infty$ and $\alpha > \max\{0, 1 - 3/p\}$, every Schwartz function satisfies

$$\|Uf\|_{L^p(\mathbb{R}^3\times[1,2])} \le C_{p,\alpha}\|J^\alpha f\|_{L^p(\mathbb{R}^3)}.$$

Corollary 10.6 · p. 158

Corollary 10.7 — Maximal half-waves and convergence to the initial data

Let $3 \le p < \infty$ and $s > 1 - 2/p$. For Schwartz functions,

$$\left\| \sup_{0<t<1} |Uf(\cdot,t)| \right\|_p \le C_{p,s}\|J^s f\|_p.$$

The family has a bounded maximal extension to $W^{s,p}(\mathbb{R}^3) = \{f \in \mathcal{S}' : J^s f \in L^p\}$. In that extension, $Uf(x,t) \to f(x)$ almost everywhere as $t \downarrow 0$, for every $f \in W^{s,p}$.

Corollary 10.7 · p. 160

Theorem 11.1 — Maximal Bochner–Riesz bounds and almost-everywhere summation

Let B_R^δ have multiplier $(1 - |\xi|^2/R^2)_+^\delta$, and put $B_*^\delta f = \sup_{R>0} |B_R^\delta f|$. If $3 \le p < \infty$ and $\delta > 1 - 3/p$, then

$$\|B_*^\delta f\|_p \le C_{p,\delta}\|f\|_p \qquad (f \in \mathcal{S}(\mathbb{R}^3)).$$

There is a bounded maximal extension to L^p; in this extension, $B_R^\delta f \to f$ almost everywhere as $R \to \infty$, for every $f \in L^p$. In particular, every $\delta > 0$ is allowed at $p = 3$.

Theorem 11.1 · pp. 160–161

Corollary 11.2 — The full strict nonmaximal Bochner–Riesz range

For $1 \le p \le \infty$, with $1/\infty = 0$, put

$$\delta_{\mathrm{BR}}(p) = \max\{3|1/p - 1/2| - 1/2, 0\}.$$

If $\delta > \delta_{\mathrm{BR}}(p)$, then B_R^δ extends boundedly to $L^p(\mathbb{R}^3)$, with

$$\|B_R^\delta f\|_p \le C_{p,\delta}\|f\|_p \qquad (R > 0)$$

uniformly in the radius. The following proof also gives convergence in L^p when $p < \infty$. This is a range for the individual linear operators, not an enlargement of the maximal range in Theorem 11.1.

Corollary 11.2 and proof · pp. 161–162

References on the arrows

Unprefixed theorem, lemma, section and equation numbers refer to Critical local smoothing for the three-dimensional wave equation. External inputs use the following keys.

- GWZ20 Larry Guth, Hong Wang, and Ruixiang Zhang — A sharp square function estimate for the cone in R3: The manuscript extends the cone wave-envelope estimate to Hilbert-valued and weighted forms for cylinder kinetic and angular-memory bounds. Annals of Mathematics 192 (2020), 551–581.
- RW25 Kevin Ren and Hong Wang — Furstenberg sets estimate in the plane: The discretized planar Furstenberg estimate is converted to a probability form for zero-cost exclusion and conditional incidence/projection. arXiv:2308.08819v3, January 19, 2025.
- BHS19 David Beltran, Jonathan Hickman, and Christopher D. Sogge — Sharp local smoothing estimates for Fourier integral operators: Implications from local smoothing to maximal half-waves and linear/maximal Bochner–Riesz estimates. arXiv:1812.11616v2, September 5, 2019.

Each citation gives the result and pages. When printed pagination differs from the PDF position, both are shown. GitHub previews do not automatically jump to the cited page.

2. Proof of Theorem 1.1 — Returning from the model to the physical wave

Proof target : Theorem 1.1 · p. 1

Proof route. Transfer the cylinder estimate to the round model, then obtain an estimate on each annulus $|\xi| \asymp H^{-1}$. Initial regularity and synthesis from terminal masses require separate arguments. A positive Sobolev loss finally makes the frequency sum converge.



The physical connection to critical smoothing

Open figure ↗ TeX source ↓

1. Prove regularity on the initial slice

Localize the negative half-wave $Wg(x,\tau) = e^{-i\tau|D|}g(x)$ to finitely many angular charts and bounded spatial regions. In null coordinates

$$t = \tau + x_3, \quad b = (x_1, x_2), \quad y = \tau - x_3, \qquad \rho = (|\xi| + \xi_3)/2, \quad A = \xi_\perp/(2\rho),$$

the velocities become $(A, |A|^2)$, but the original initial slice is $y = -t$, rather than $t = 0$. The uniform kernel truncation in Lemma 10.2 permits restriction of the input to the predecessor set E of a regularity test. Lemma 10.3 bounds its volume by $C\Lambda^{C_1} r^4 f^{1-\eta}$, where f denotes relative test thickness, not the input function. The gradient lower bound for the restricted polynomial also handles nonround tests.

With $B = \|g\|_\infty$ and $e \lesssim \|g\|_2^2$, Proposition 10.4 gives initial regularity constant $\kappa = C_{\eta,\gamma} H^{-\gamma} B^2$, for every $\gamma > 0$. This verifies the model hypothesis from the original datum.

Lemmas 10.2–10.3; Proposition 10.4 · pp. 153–156

2. Synthesize the cubic sum of terminal masses

Let $m_{j,Q}$ be the energy assigned to a spatial H-cube in a terminal time interval of length H. The test weights are comparable to one, and assignments within each interval sum to at most its row energy. Lemma 10.5 and Theorem 9.1 give, for arbitrarily small positive σ, ζ,

$$\int |v|^3 \lesssim H^{-C_4\sigma} H^{-1/2} \sum_{j,Q} m_{j,Q}^{3/2} + \text{negligible error}, \qquad H^{-1/2} \sum_{j,Q} m_{j,Q}^{3/2} \lesssim H^{-100\eta-\zeta} e\sqrt{\kappa}.$$

Consequently,

$$\int |v|^3 \lesssim H^{-100\eta-\zeta-\gamma/2-C_4\sigma} B \|g\|_2^2.$$

Choose a desired loss first, then take $\eta, \zeta, \gamma, \sigma$ sufficiently small. Evolution copies energy into descendant time intervals; these descendants are not mutually orthogonal pieces of the initial datum.

Lemma 10.5; (10.22)–(10.23) · pp. 156–157

3. Decompose amplitudes and sum frequencies

Apply spatial and dyadic amplitude decompositions to the input. Each amplitude piece satisfies $B_\nu \|g_\nu\|_2^2 \le 2\|g_\nu\|_3^3$, and the logarithmic number of pieces is absorbed into an arbitrarily small power loss. This proves Proposition 10.1, uniformly for smooth symbol families on a fixed annulus:

$$\|W_H g\|_{L^3_{x,\tau}} \le C_\delta H^{-\delta} \|g\|_3 \qquad (\delta > 0).$$

Set $h = J^\varepsilon f$, $H = 2^{-n}$, and $\delta = \varepsilon/2$. Inserting $J^{-\varepsilon}$ into the annular symbol gives summable terms $2^{-n\varepsilon/2}\|h\|_3$. Uniformly integrable kernels handle low frequencies, and complex conjugation restores the positive sign.

Proposition 10.1 and proof; §10.5 · pp. 152, 157–158

3. Proof of Theorem 3.6 — Entropy excess in the cylinder model

Proof target : Theorem 3.6 · p. 18

Theorem 3.6 — Cylinder growth exponents

Consider the classical and hybrid cylinder experiments of Definitions 3.1–3.3. Classical velocities are (X, X^2, N). The hybrid model retains classical parabolic base variables and one-dimensional Schrödinger evolution in the normal variable. Tests use position and velocity windows after subtracting polynomial shears, with weight $w = r^{3+\eta} f^{1-\eta}$, $0 < \eta < 1$. The angular width is $r > 0$, the normal width is $f > 0$, and hybrid tests require $f \geq (H/\ell)^{1/2}$. Impose initial mass $e > 0$ and regularity $\mu(Q) \leq \kappa w(Q)$. At the final cut of length s, assign masses m_λ to tests, with assignments within each interval dominated in sum by its row energy.

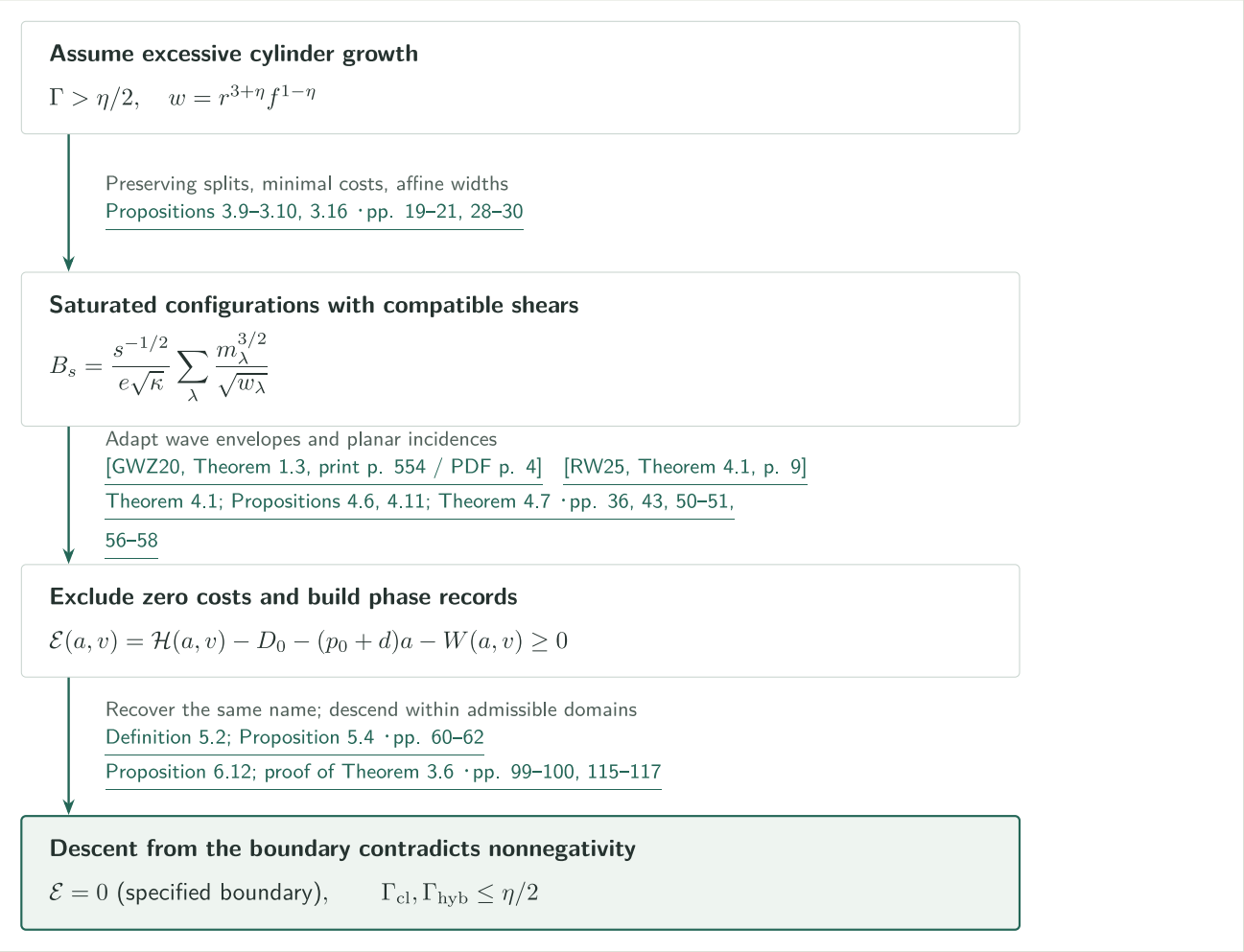
$$B_s = \frac{s^{-1/2}}{e\sqrt{\kappa}} \sum_\lambda \frac{m_\lambda^{3/2}}{\sqrt{w_\lambda}}.$$

Under the fixed finite operator-cut and polynomial support, density, and negligible-error conventions, the supremal upper $\log_{1/s}$ growth exponents over admissible setups satisfy

$$\Gamma_{\mathrm{cl}} \leq \eta/2, \qquad \Gamma_{\mathrm{hyb}} \leq \eta/2.$$

The setup, number of cuts, and error tolerances are fixed before the inner scale limit.

Definitions 3.1–3.3; Theorem 3.6 · pp. 14–18



Extremal cylinder configurations and the entropy contradiction

Open figure ↗ TeX source ↓

1. Preserving extremality forces compatible shears

Assume growth beyond the asserted bound. Propositions 3.9–3.10 show that ordinary regularity splits preserving the extremal exponent must saturate the energy and regularity budgets at the exponent level. Comparing tests at different cuts then controls their shear coefficients and permits selection of minimal shear costs. Proposition 3.16 restricts to a short depth interval and renormalizes, obtaining $u(i) = J(1 - i)$ and affine normal-width exponents. The extraction preserves enough compatibility to recover earlier frames from later finite records; selecting large masses independently at each depth would not suffice.

Propositions 3.9–3.10, 3.16 · pp. 19–21, 28–30

2. External inputs exclude zero costs and supply conditional projections

The wave-envelope theorem of [GWZ20] concerns scalar functions near the cone. Theorem 4.1 derives a Hilbert-valued version by Gaussian averaging and a weighted version by summing tiles. The kinetic estimate for parabolic rays in Lemma 4.2 and the angular-memory estimate in Proposition 4.3 lead to Proposition 4.6, excluding hybrid zero costs when the hybrid exponent strictly exceeds the classical one.

Theorem 4.7 converts the discretized Furstenberg theorem of [RW25] into a probability-measure statement by point–line duality and sampling. Nonconcentration exponents b for the line family and a along its lines give union covering exponent

$$F(a,b) = a + \min\{1, b, (a+b)/2\}.$$

It enters the classical zero-cost exclusion in Proposition 4.11 and the subsequent conditional incidence and projection estimates. The probability and Hilbert-valued extensions are proved in this manuscript, rather than attributed to the external theorems themselves.

[GWZ20, Theorem 1.3, print p. 554 / PDF p. 4]

[RW25, Theorem 4.1, p. 9]

Theorem 4.1; Propositions 4.6, 4.11; Theorem 4.7 · pp. 36, 43, 50–51, 56–58

3. Nonnegativity conflicts with descent for one finite phase record

The canonical name $C(a,v)$ of Definition 5.2 records time, shear coefficients, base position and direction, and dyadic cells of the residual normal phase at time depth a and angular resolution v. Subtract from its normalized entropy $\mathcal{H}(a,v)$ the initial ratio $D_0 = \lim \log_{1/s}(e/\kappa)$, the saturated mass baseline $(p_0 + d)a$, and the test-weight exponent $W(a,v)$. Then

$$\mathcal{E}(a,v) = \mathcal{H}(a,v) - D_0 - (p_0 + d)a - W(a,v) \geq 0.$$

Here p_0 is the manuscript's mass exponent p, distinguished from the L^p exponent. Proposition 5.4 gives equality only at specified terminal and boundary resolutions. Hybrid use is restricted to normal-width exponent $w < 0$; boundary equality is not available at arbitrary resolutions.

Section 6 collects local inequalities into the admissible motions of Proposition 6.12. Section 7 builds backward paths from equality boundaries, staying inside the domains of the applicable inequalities. A strictly positive drop contradicts $\mathcal{E} \geq 0$. Unit-cost boundaries, intervals with no angular entropy growth, and quadratic versus linear shears require separate cases. This overview does not independently verify every case of that argument.

Definition 5.2; Proposition 5.4 · pp. 60–62

Proposition 6.12; proof of Theorem 3.6 · pp. 99–100, 115–117

4. Proof of Theorem 9.1 — Transferring thin shapes and excluding round configurations

Proof target : Theorem 9.1 · p. 133

Theorem 9.1 — Round-cone growth exponents

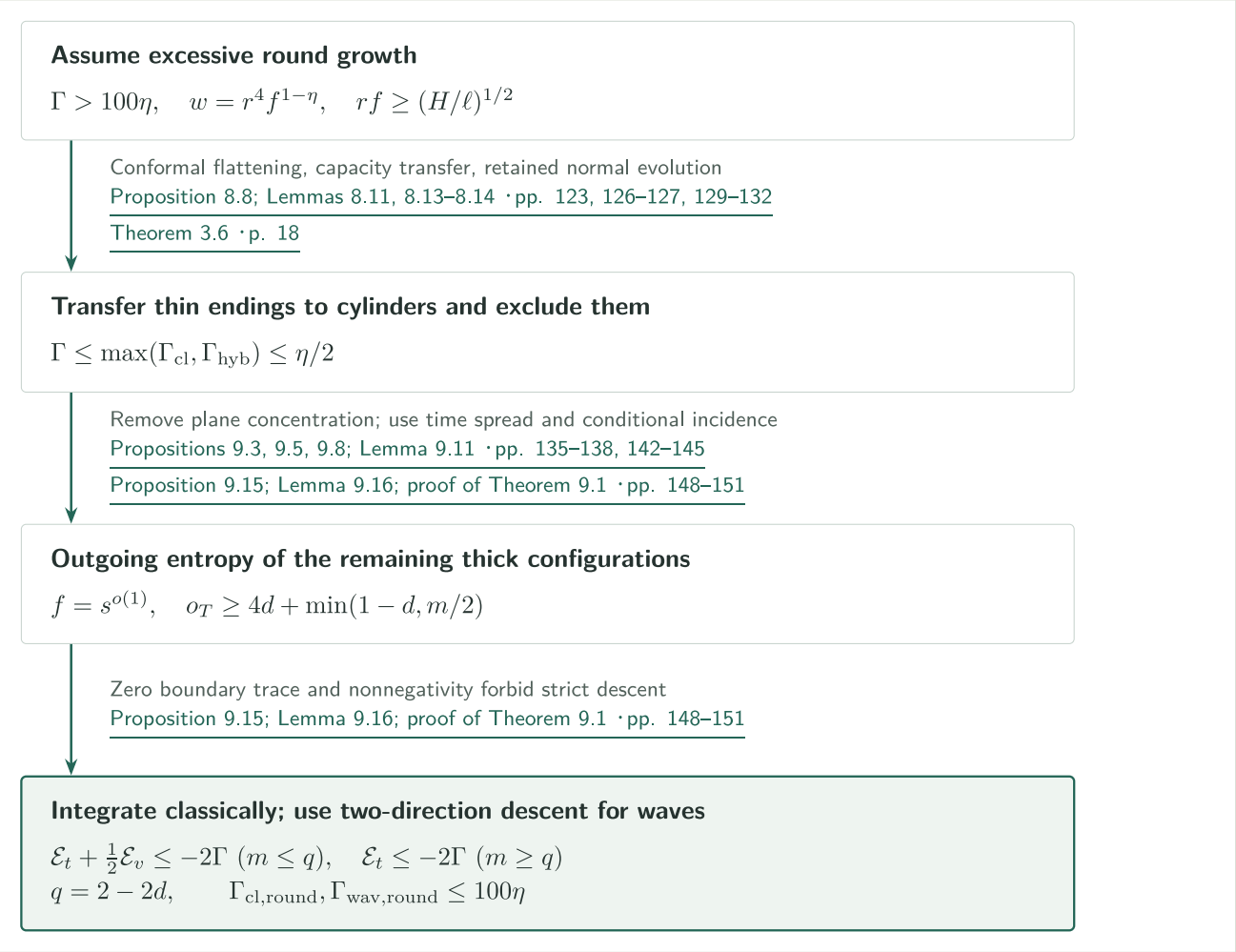
Consider the classical and wave experiments of Definitions 8.1–8.2, with velocities $(A, |A|^2)$, $A \in \mathbb{R}^2$. At time length ℓ, tests have angular width r, position widths $\ell r, \ell r^2$, and may have relative thickness $0 < f \le 1$ near a hyperquadric. Wave tests satisfy $rf \ge (H/\ell)^{1/2}$. Use initial regularity with weight $w = r^4 f^{1-\eta}$, and the same normalized functional B_s as above.

For every $0 < \eta < 1$,

$$\Gamma_{\mathrm{cl,round}} \le 100\eta, \qquad \Gamma_{\mathrm{wav,round}} \le 100\eta.$$

The bounds also hold with a fixed finite list of admissible row contractions, arbitrary separable Hilbert multiplicity, and the model's finite-power support and error conventions.

Definitions 8.1–8.2; Theorem 9.1 · pp. 117–118, 133



Thin-shape reduction and the remaining round configurations

Open figure ↗ TeX source ↓

1. Transfer thin endings to cylinders

Proposition 8.8 reduces saturated configurations with a positive limiting terminal-thickness exponent to cylinders. It gives $\Gamma \leq \Gamma_{\mathrm{cl}}$ classically, and $\Gamma \leq \max\{\Gamma_{\mathrm{cl}}, \Gamma_{\mathrm{hyb}}\}$ for waves. Group tests near a common hyperquadric, flatten it in a conformal chart, and transfer both initial regularity and terminal capacities. Freezing fine base variables must retain the normal quantum evolution, which is why the hybrid cylinder model is needed. The input/output weight comparison of Lemma 8.13 accounts for cancellation of the normal rescaling factors.

Proposition 8.8; Lemmas 8.11, 8.13–8.14 · pp. 123, 126–127, 129–132

2. Obtain angular transversality for the remaining configurations

After Theorem 3.6 excludes thin endings, saturated configurations have $f = s^{o(1)}$. The classical case is closed first. For a wave configuration strictly exceeding that classical exponent, Proposition 9.3 fixes the angular width at the uncertainty scale. The plane-slab estimate in Proposition 9.5 and Lemma 9.11 remove conditional plane concentration. Proposition 9.8 gives a nonnegative phase-record entropy excess, zero on $v = (1 - a)/2$.

Propositions 9.3, 9.5, 9.8; Lemma 9.11 · pp. 135–138, 142–145

3. Two-direction descent of the outgoing entropy

Proposition 9.15 combines time nonconcentration with transverse angular samples to give outgoing entropy rate

$$o_T \geq 4d + \min\{1 - d, m/2\}.$$

Four transverse directions supply $4d$; conditional planar incidence gives the improvement. Classically, integration gives $D(1, 0) \geq 1 + 3d$, contradicting the terminal upper bound $D(1, 0) \leq 1 + 3d - 2\Gamma$.

For waves put $t = 1 - a$ and $q = 2 - 2d$. Then

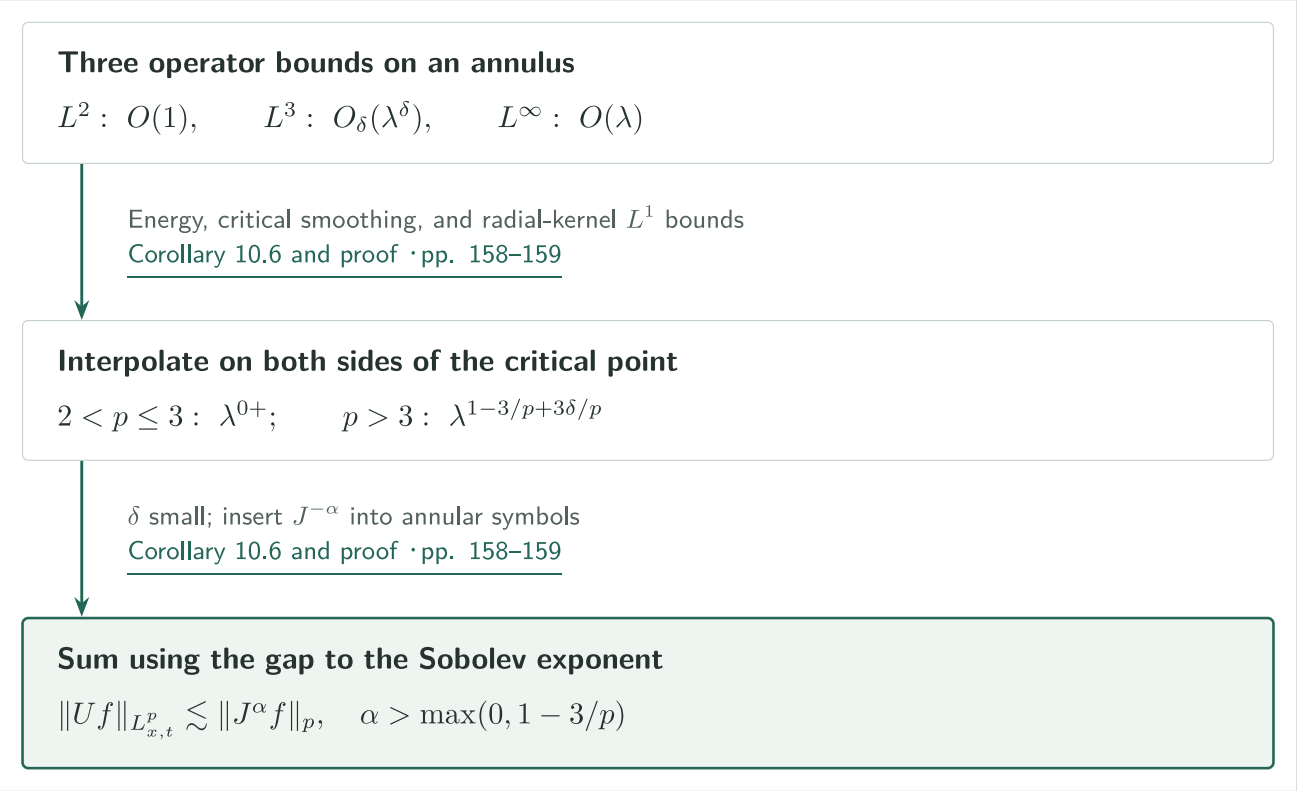
$$\mathcal{E}_t + \tfrac{1}{2}\mathcal{E}_v \leq -2\Gamma \quad (m \leq q), \qquad \mathcal{E}_t \leq -2\Gamma \quad (m \geq q).$$

Monotonicity of m in t at fixed v permits switching between these directions without losing the negative decrease. Lemma 9.16 contradicts nonnegativity and the zero boundary trace. This supplies the model loss 100η used in Theorem 1.1.

Proposition 9.15; Lemma 9.16; proof of Theorem 9.1 · pp. 148–151

5. Proof of Corollary 10.6 — Interpolating L^2, L^3, L^∞

Proof target : Corollary 10.6 · p. 158



Interpolation and frequency summation for other exponents

Open figure ↗ TeX source ↓

1. Interpolate on an annulus and use the strict inequality to sum

For a smooth annular projection P_λ, $\lambda \ge 1$, the operator norms are $O(1)$ from L^2 to spacetime L^2, $O_\delta(\lambda^\delta)$ from L^3 to spacetime L^3, and $O(\lambda)$ from L^∞ to spacetime L^∞. The last follows by integrating the radial three-dimensional kernel in absolute value.

Interpolation gives an arbitrarily small positive power for $2 < p \le 3$, and $\lambda^{1-3/p+3\delta/p}$ for $p > 3$. Choose δ so that this exponent is below α, insert $J^{-\alpha}$, and sum geometrically. The appended estimate for independent displacement and velocity data follows from both signs and the order -1 velocity multiplier:

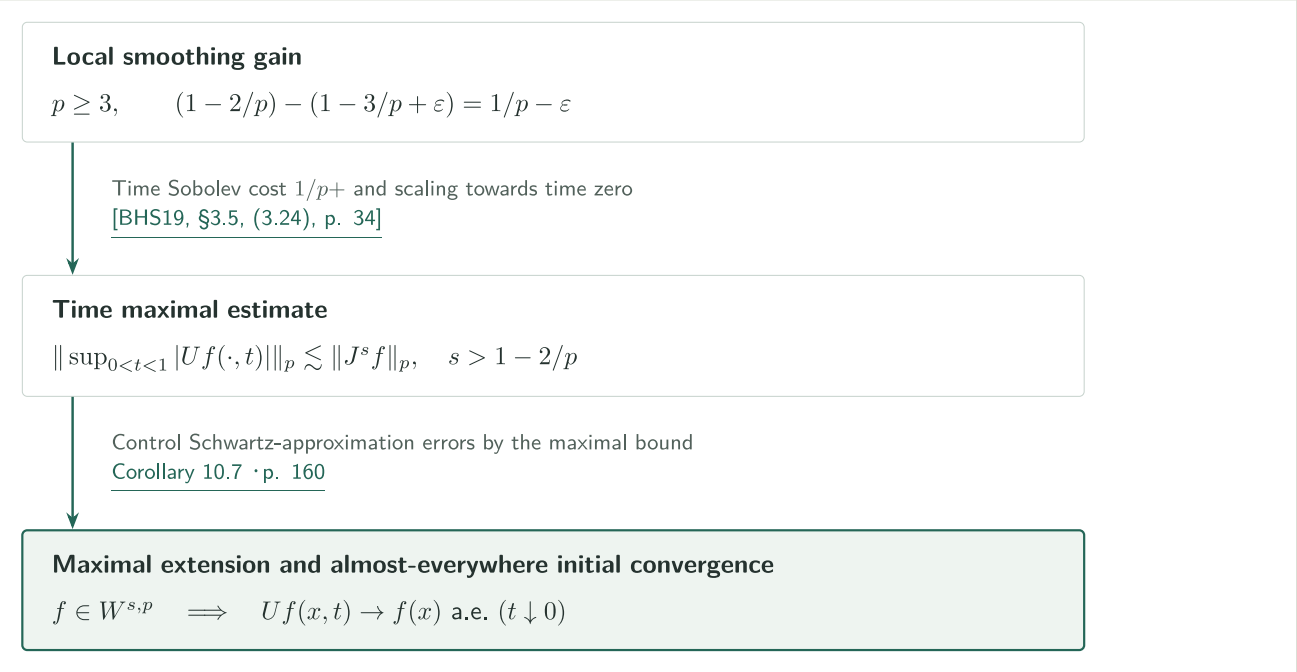
$$\|u\|_{L^p_{x,t}} \lesssim \|J^\alpha u_0\|_p + \|J^{\alpha-1} u_1\|_p.$$

At low frequency retain the combined multiplier $\sin(t|\xi|)/|\xi|$.

Corollary 10.6 and proof · pp. 158–159

6. Proof of Corollary 10.7 — Time Sobolev embedding and density

Proof target : Corollary 10.7 · p. 160



Maximal half-waves and initial convergence

Open figure ↗ TeX source ↓

1. Take the time supremum and control approximation errors

For $p \geq 3$, the gain over the fixed-time loss $1-2/p$ is $1/p-$. The implication in [BHS19, §3.5, (3.24)] combines time Sobolev embedding, costing $1/p+$, with scaling to give the $0<t<1$ maximal estimate when $s > 1-2/p$. Corollary 10.6 supplies its hypothesis; one is not simply quoting the older paper's established exponent range.

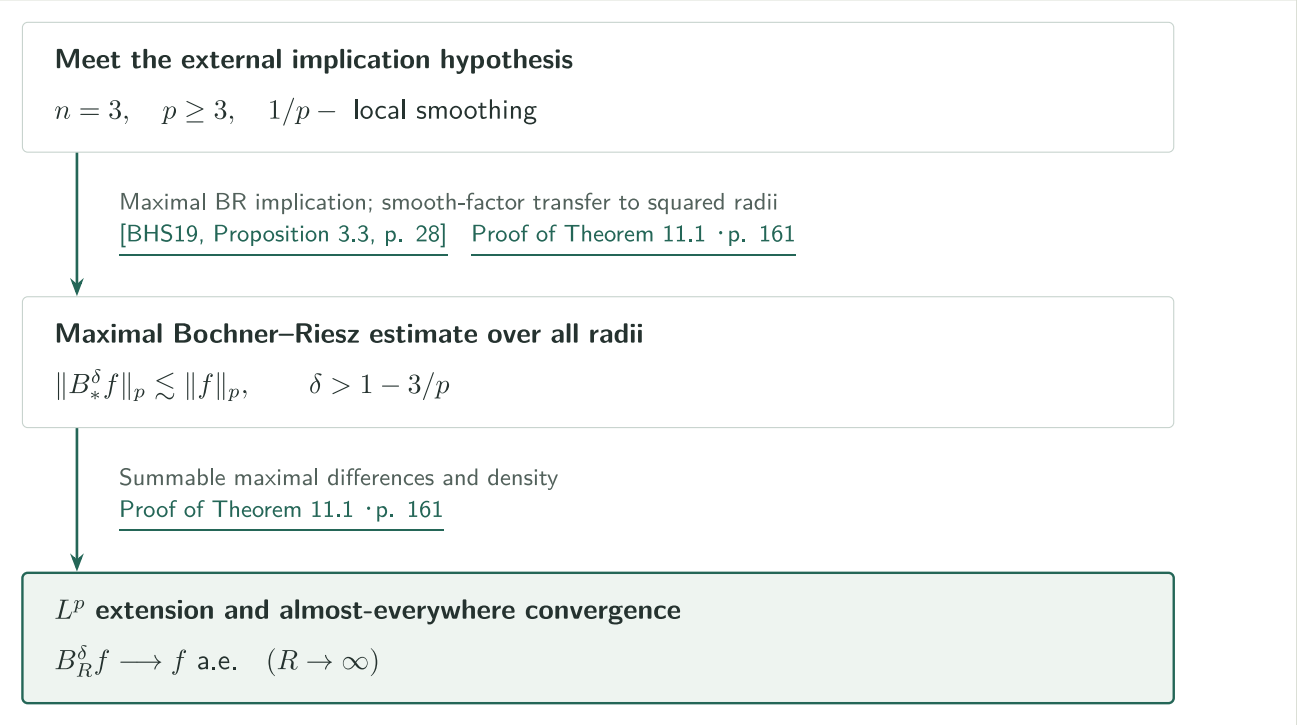
Schwartz data converge uniformly as $t \downarrow 0$. Approximate in $W^{s,p}$, then use the maximal estimate and Chebyshev's inequality to make the exceptional limsup set have measure zero. At $p=3$ the maximal conclusion requires $s > 1/3$, unlike the spacetime estimate with every positive loss.

[BHS19, §3.5, (3.24), p. 34]

Corollary 10.7 · p. 160

7. Proof of Theorem 11.1 — From local smoothing to maximal Bochner–Riesz

Proof target : Theorem 11.1 · pp. 160–161



The direct input for maximal Bochner–Riesz estimates

Open figure ↗ TeX source ↓

1. Match the threshold and multiplier convention

[BHS19, Proposition 3.3] assumes $1/p-$ local smoothing for $p \geq 2n/(n-1)$. With $n = 3$ and $p \geq 3$, Corollary 10.6 meets this hypothesis and the required order becomes $\delta > 1 - 3/p$. Its multiplier $(1 - |\xi|/R)_+^\delta$ is related to the squared-radius convention by the smooth factor $(1 + |\xi|/R)^\delta$ near the boundary and a smooth interior remainder. Their Schwartz kernels and the Hardy–Littlewood maximal operator transfer the bound for the supremum over all radii.

[BHS19, Proposition 3.3, p. 28]

Proof of Theorem 11.1 · p. 161

2. Construct the maximal extension and almost-everywhere sum

Choose Schwartz approximants whose successive L^p differences are summable. The maximal functions of their differences are also summable in L^p, defining an extension uniform over all radii at almost every point. Then

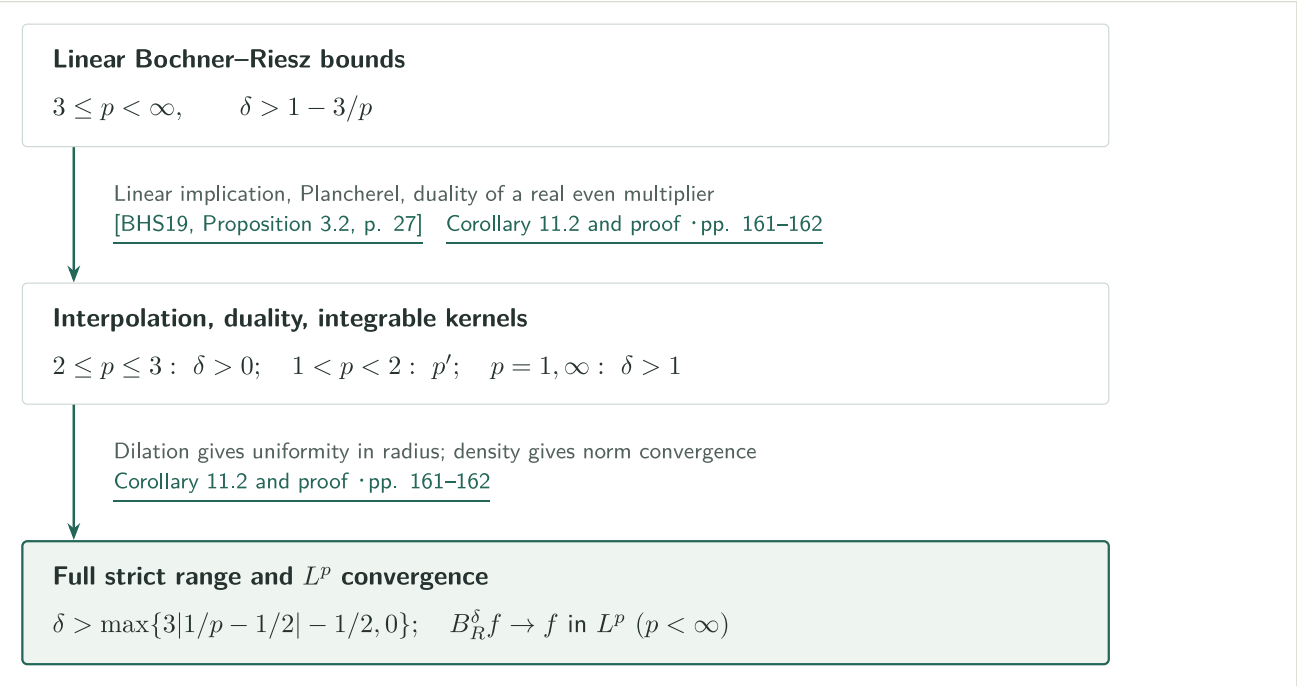
$$\limsup_{R \to \infty} |B_R^\delta f - f| \leq B_*^\delta (f - g) + |f - g|$$

transfers convergence for Schwartz g to arbitrary L^p data. No Sobolev regularity of the input is required.

Proof of Theorem 11.1 · p. 161

8. Proof of Corollary 11.2 — Interpolation and duality for linear means

Proof target : Corollary 11.2 and proof · pp. 161–162



The complete nonmaximal Bochner–Riesz range

Open figure ↗ TeX source ↓

1. Complete the exponent range and norm convergence

[BHS19, Proposition 3.2] and the same smooth-factor transfer give the linear bounds for $3 \le p < \infty$, $\delta > 1 - 3/p$. At fixed $\delta > 0$, interpolate the $p = 3$ bound with Plancherel to fill $2 \le p \le 3$. Duality of the real even multiplier supplies $1 < p < 2$. At $p = 1, \infty$, the condition $\delta > 1$ makes the kernel decay $(1 + |x|)^{-2-\delta}$ integrable. Dilation gives constants uniform in the radius.

For $p < \infty$, first prove L^p convergence for Schwartz functions with compact Fourier support; uniform linear operator bounds and density then extend it. This duality argument is not applied to the maximal operator.

[BHS19, Proposition 3.2, p. 27]

Corollary 11.2 and proof · pp. 161–162

9. Which papers supply which steps

Source and result

Guth–Wang–Zhang, Theorem 1.3

Used at

Theorem 4.1, Lemmas 4.2–4.4, Proposition 4.6

Role and hypotheses

Cone wave envelopes lead to Hilbert-valued and weighted estimates, then cylinder angular memory

Checking scope

External statement and the manuscript's extension/application route compared; complete external proof excluded

---

Source and result

Ren–Wang, Theorem 4.1

Used at

Theorem 4.7, §§4.5, 5–6, Proposition 9.15

Role and hypotheses

Covering lower bounds for nonconcentrated point–line configurations become conditional incidence estimates

Checking scope

External statement, probability conversion, and central uses compared; all conditional lemmas not independently verified

Source and result

Beltran–Hickman–Sogge, §3.5 (3.24), Propositions 3.2–3.3

Used at

Corollary 10.7, Theorem 11.1, Corollary 11.2

Role and hypotheses

$1/p-$ smoothing implies maximal half-wave and linear/maximal BR bounds

Checking scope

Exponent hypotheses and the multiplier-convention transfer compared

Bochner–Riesz multipliers in three dimensions in catalogue 078 is cited on p.162 as a different proof of the same nonmaximal range, explicitly not an input to this deduction. No direct citation to either catalogue 074 manuscript was found in this manuscript's bibliography. Section 11.1 derives spherical restriction and Kakeya maximal estimates through a different external chain.

Corollary 11.2, final paragraph; §11.1 · p. 162

10. Return to the sources

- Definitions 3.1–3.3; Theorem 3.6 · pp. 14–18 — Cylinder regularity, assignments, and growth exponents
- Definition 5.2; Proposition 5.4 · pp. 60–62 — Phase names recording shears and endpoint recovery
- Proposition 8.8; Lemmas 8.11, 8.13–8.14 · pp. 123, 126–127, 129–132 — The thin-shape transfer to cylinders
- Proposition 9.15; Lemma 9.16; proof of Theorem 9.1 · pp. 148–151 — Outgoing entropy and the final two-direction contradiction
- Lemmas 10.2–10.3; Proposition 10.4 · pp. 153–156 — Regularity on the original initial slice
- Proposition 10.1 and proof; §10.5 · pp. 152, 157–158 — From annular bounds to Sobolev summation
- Corollary 10.6 and proof · pp. 158–159 — Other exponents and independent initial data
- Corollary 10.7 · p. 160 — Time maxima and initial convergence
- Corollary 11.2 and proof · pp. 161–162 — Distinguishing maximal and nonmaximal BR ranges

Reading focused on the statements, model definitions, extremal configurations, phase records and entropy endpoint conditions, thin-shape reduction, final round-model contradiction, physical initial regularity, frequency summation, and proofs of the numbered consequences. The quantitative GWZ and Ren–Wang inputs and the BHS maximal implications were compared with their statements and application hypotheses. This is not an independent verification of every lemma and case in the 165-page manuscript. In particular, checking of conditional-information transfers and boundary paths in §§5–7 and all conformal-transfer error calculations in §8 is limited.

The manuscript's deductions of spherical restriction, Kakeya maximal bounds, and the dimension of compact Kakeya sets in §11.1 (p.162) were read, but source comparison of the external Tao and Wolff implications is outside this overview's scope. Their checking status is distinct from that of the numbered results above. No expert review or certification of the complete proof is claimed.